JOURNAL OF CATALYSIS 137, 285–305 (1992)

# Development of Molybdena Catalysts Supported on γ-Alumina Extrudates with Four Different Mo Profiles: Preparation, Characterization, and Catalytic Properties

M. A. GOULA,* CH. KORDULIS,* A. LYCOURGHIOTIS,*,[1] AND J. L. G. FIERRO†

*Department of Chemistry, University of Patras–Institute of Chemical Engineering and High Temperature Processes, GR-26110, Patras, Greece; and †Instituto de Catalisis y Petroleoquimica, C.S.I.C., Campus UAM, Cantoblanco, 28006 Madrid, Spain

Received January 2, 1992; revised April 8, 1992

The main goal of this work is to prepare, characterize, and determine the catalytic properties of molybdena supported γ-alumina extrudates with four Mo profiles. Concerning preparation, a procedure was established allowing us to prepare (both axially and radially) egg-shell, egg-white, egg-yolk, and uniform profiles with the same, relatively high, Mo loading. The preparation of the egg-shell and uniform profiles was achieved by impregnating γ-alumina extrudates with acidic and alkaline ammonium heptamolybdate solution, respectively. Moreover, it was found that an egg-white (egg-yolk) profile may be achieved from an egg-shell (uniform) profile by successive pore volume or simple nondry impregnations of the Mo-supported extrudates with $NH_4OH$ aqueous solutions. A qualitative mechanism, based on the relative rates of desorption and diffusion of the $MoO_4^{2-}$ ions occuring in the $NH_4OH$ impregnation, was developed to interpret the influence of desorption time, concentration of $NH_4OH$ solution, drying, and mode of impregnation on the characteristics of the egg-white and egg-yolk profiles obtained. The physicochemical characterization of the Mo/γ-alumina extrudates for which radial profiles have been achieved, done by using a number of techniques, showed a progressive increase of the "Mo supported–support" interactions and Mo dispersion following the order egg-yolk < uniform < egg-white < egg-shell. A similar trend (uniform < egg-yolk < egg-white < egg shell) was obtained for the number of active sites as estimated by the amount of the adsorbed NO. The trends mentioned above were related with the values of the preparative parameters used for obtaining each profile. Kinetic experiments were done, using the hds of thiophene as a probe reaction, over the characterized samples being in the form of extrudates and powders produced by crushing the extrudates. It was found that hds activity was mainly determined by the number and the quality of active centers and not by the type of Mo profile, though these suggested the presence of no significant diffusional effects. The relative yield of butane, produced by the hydrogenation of the unsaturated hydrocarbons formed during hds, increased with the distance of the maximum of the Mo profile from the periphery of the extrudate to its center. Finally, it is important to note that the most active radial profile proved to be the egg-white for hds and the egg-yolk for hydrogenation. 

## INTRODUCTION

In the framework of a research program recently undertaken in our laboratory, a very simple technique was developed allowing the determination of axial macrodistributions in extrudates (*1*). Using this technique we studied in detail the influence of the impregnation parameters on the characteristics of the Mo axial profiles obtained on the γ-alumina extrudates. It was found that a decrease in pH as well as an increase in the concentration of the molybdate solutions, of the impregnation temperature, and of the rate of drying caused a progressive transformation of the Mo profile from uniform to egg-shell. The opposite trend was obtained by doping γ-alumina extrudates with $F^-$ ions or by using $NH_4F$, $H_3PO_4$, and citric acid as competitors. An increase of

[1] To whom correspondence should be addressed.



0021-9517/92 $5.00

the impregnation time until a critical value favoured the progressive transformation of the Mo profile from egg-shell to uniform. An additional increase in the impregnation time caused the opposite effect. Finally, no considerable effect on the Mo profile was observed by changing the volume of the impregnating solution. Most of the above results, being in agreement with the literature (*2, 3*), were explained on the basis of equations derived adopting a very simple macrodistribution model (*4*). The equations derived showed that similar axial and radial Mo profiles should be expected under the same experimental conditions, and this prediction was experimentally confirmed. Moreover, the above study showed that only two Mo profiles, namely, egg-shell and uniform, may be obtained by regulating the values of the formentioned impregnating parameters. It is obvious that alternative methods should be developed in order for egg-white and egg-yolk profiles to be achieved.

The present paper describes the continuation of our effort to obtain and study all types of $Mo/\gamma\text{-}Al_2O_3$ axial and radial profiles. Concerning the axial profiles we examined the influence of the impregnating parameters on the amount of Mo deposited on $\gamma$-alumina. We have also attempted to prepare *all* $Mo/\gamma\text{-}Al_2O_3$ macrodistributions. Based on the results reported in a previous publication (*1*), as well as on the results obtained in the present study on axial profiles, we attempted to prepare all the $Mo/\gamma\text{-}Al_2O_3$ radial profiles. EDX microanalysis was used to investigate the profile type achieved. The profiles were characterized in order to examine whether the change in the preparative parameters, necessary to obtain different radial macrodistributions, influenced the structure and the texture of the active phase achieved in each profile (dispersity, interaction with the support, etc.). This type of information is of importance, for the design of catalyst preparation with specific macrodistribution. In this process, the "microscopic characteristics" of the active phase, in relationship with the number and the quality of the active centers, should not be ignored. The characterization of the oxidic phase included measurements of the specific surface area (SSA) using $N_2$ adsorption as well as the determination of the dispersity and the "$MoO_3$ phase–support interactions" by X-ray photoelectron spectroscopy (XPS) and temperature programmed reduction (TPR), respectively. The active surface in the reduced Mo state was determined using NO adsorption.

Finally, using the hydrodesulfurization of thiophene as a probe reaction, it was attempted to relate the catalytic activity and selectivity with the radial profiles achieved.

## EXPERIMENTAL

### Substances–Solutions

$\gamma$-alumina pellets of 7 mm length and 3.2 mm diameter were used in the present study. The composition of the pellets was $\gamma\text{-}Al_2O_3$, 97%; $SiO_2$, 0.05%; and $Na_2O$, 0.7%. The specific surface area (SSA) and the average pore diameter were respectively 120 $m^2\ g^{-1}$ and 110 Å. The water pore volume was 0.35 $cm^3\ g^{-1}$.

Ammonium heptamolybdate, $(NH_4)_6\ Mo_7O_{24} \cdot 4H_2O$, obtained from Riedel de Haen (99%), was used for the preparation of the molybdate aqueous solutions. The pH of these solutions was adjusted at pH values lower or higher than the point of zero charge of $\gamma\text{-}Al_2O_3$, being equal to 5.3, by adding $HNO_3$ or $NH_4OH$, as needed.

### Axial Profiles

#### *Preparation*

The preparation of egg-shell and uniform axial profiles was done following the procedure described in our previous paper (*1*). In order to prepare egg-white and egg-yolk axial profiles a procedure similar to that used for the preparation of egg-shell and uniform axial profiles, respectively, was followed. The main difference is that following impregnation with AHM solution and drying at 120°C for 2 h we have done either successive dry impregnations with 0.1 *N* $NH_4OH$

followed by drying at 10°C for 2 h or a simple nondry impregnation with 20 ml $NH_4OH$ (0.1 *N*, pH = 10) for a time period (1–12 h) at 25°C followed by filtration and drying at 120°C for 2 h. It was found that during the impregnations with $NH_4OH$-supported Mo species were desorbed from the support surface.

*Determination of Axial Profiles and Total $Mo^{(VI)}$ Amount Deposited on the $\gamma$-Alumina Surface*

The dried extrudates were divided into 10 slices of equal thickness (0.7 mm) using a cutting tool made in the laboratory (*1*). The slices located at the same distance from the center of the cylinders were then separated and weighed. Molybdena was extracted by treating each sample (ca. 0.2 g) with 2 $cm^3$ of an ammonia solution (0.1 N, pH = 10) for 17 h. Following filtration the extracted Mo was determined spectrophotometrically at 490 nm (Varian Carry 219) (*5*). In all cases the total molybdenum extracted was almost equal to that adsorbed during impregnation.

By using this technique, it was possible to draw "*N* vs *X*" curves, i.e., of the Mo loading ($\mu$mol $m^{-2}$), *N*, determined in the slice at distance *X* from an edge of the extrudates. Furthermore, we could determine also the total $Mo^{(VI)}$ amount deposited on the $\gamma$-alumina surface.

## Radial Profiles

*Kinetics of Desorption of Supported $Mo^{(VI)}$ Species*

The experiments concerning the axial profiles showed that egg-white and egg-yolk profiles may be obtained starting from egg-shell and uniform profiles, respectively, and desorbing the $Mo^{(VI)}$-supported species located in the periphery of the extrudates by impregnation with $NH_4OH$ aqueous solutions. Knowledge of the kinetics of desorption of the $Mo^{(VI)}$-supported species is anticipated to be helpful for the preparation of the corresponding radial profiles.

In order to study the kinetics with respect to the preparation of egg-yolk profile from uniform profile, a uniform profile was prepared by impregnating 20 uncovered (*1*) extrudates (ca. 2 g) in 20 ml of AHM aqueous solutions, ($C_0$ = 1.5 *M*, pH = 10) for reduced impregnation time, $\tau_i$, equal to 10 ($\tau_i = t_i/t_l$, $t_i$ and $t_l$ represent respectively the impregnation time and the time required in order for the liquid imbibition to be accomplished. The latter was found equal to 6 min and 21 sec for axial and radial imbibition, respectively (*1*)). Following filtration the extrudates were dried at room temperature for 20 h and then at 120°C for 2 h. This procedure resulted in a uniform profile (*1*).

The extrudates thus prepared were impregnated in 20 ml $NH_4OH$ (0.1 *N*, pH = 10) and the suspension was rotated in a rotary evaporator in order to determine the kinetics of desorption. The Mo concentration of the aqueous phase was measured in 30-min intervals (*5*). At the same time two extrudates were removed, wiped with a tissue paper, and dried at 120°C for 2 h. Using an optical microscope the resulting radial profile was observed. It was found that as the reduced desorption time, $\tau_d$, increased the uniform profile was progressively transformed into egg-yolk profile ($\tau_d = t_d/t_l$, $t_d$ : desorption time).

A similar procedure was followed for the preparation of an egg-white profile from an egg-shell. The latter was achieved through impregnation of the extrudates in AHM aqueous solutions ($C_0$ = 0.9 *M*, pH = 5.5). Concerning the desorption of the $Mo^{(VI)}$ species, it was found that as the reduced desorption time increased the egg-shell profile was progressively transformed into egg-white.

The same type of experiments were repeated using extrudates covered by a plastic tube (*1*) for the determination of the kinetics of desorption of $Mo^{(VI)}$ species in the case of axial profiles.

*Preparation*

The procedure described below for the preparation of radial Mo profiles was established taking into account both the results

obtained from the experiments mentioned above and the recently reported results of the study on axial profiles (*1*). The close dependence of this procedure on the results mentioned above are detailed in the "Results and Discussion" section. The preparation of radial profiles involved the following steps: pretreatment of the extrudates, impregnation, desorption, and calcination.

*Pretreatment of the extrudates.* Twenty-five (25) g of uncovered extrudates were placed in a plastic netting immersed in 250 ml bidistilled water thermostated at 25°C under stirring. Following "impregnation" for 0.5 h the extrudates were removed, dried at 120°C for 2 h and then calcined at 540°C for 6 h.

*Impregnation.* Twenty-five (25) g of uncovered, already pretreated, extrudates were placed in a plastic netting immersed in 250 ml of an AHM aqueous solution of a certain concentration ($C_0 = 0.7$–$1.5\ M$) thermostatted at 25°C under stirring. The reduced impregnation time, $\tau_i$, was equal to 10, whereas the pH of the impregnating solution was equal to 4.5 and 5.5 for the preparation of egg-shell and egg-white profiles, respectively, and equal to 10.0 for the preparation of uniform and egg-yolk profiles. Following impregnation the extrudates were removed and dried first at 25°C for 20 h and then at 120°C for 2 h (uniform or egg-yolk profiles) or only at 120°C for 2 h (egg-shell or egg-white profiles). Depending on the macrodistribution desired, the impregnation procedure was performed once (uniform), twice (egg-shell), or three times (egg-white and egg-yolk). It should be noted that after the impregnation step only uniform or egg-shell profiles can be achieved with different Mo loadings, which depend on the number of impregnations and the impregnating solution concentration (*1*).

*Mo desorption.* Extrudates, on which a uniform (after three impregnations) or an egg-shell profile (after three impregnations) had been obtained in the impregnation step, were immersed in 250 ml of $NH_4OH$ solution (0.1 *N*, pH = 10). The system was rotated in a rotary evaporator for the time periods required, as determined from the kinetics of Mo desorption. Following extraction with $NH_4OH$ the extrudates were removed and dried at 120°C for 2 h. Starting with uniform or egg-shell profiles this procedure resulted in egg-yolk or egg-white profiles, respectively.

*Calcination.* All the specimens prepared were air-calcined at 300°C for 1 h and then at 550°C for 5 h.

### *Characterization*

*SEM-EDX analysis.* The SEM-EDX system used was an ISI DS-130 scanning electron microscope coupled with an Si(Li) X-ray detector and a Kevex 800II processor for energy-dispersive X-ray analysis. The extrudates studied were embedded in Araldite resin and cut by a microtome in order to get smooth cross sections of the cylinders. The classical ZAF method with Gaussian deconvolution was used for obtaining quantitative results. The analysis step was 0.3 mm on the diameter of the cross sections, whereas the corresponding time was equal to 200 s/point. Next, the analysis of the entire cross section was done.

*X-ray photoelectron spectroscopy (XPS).* Photoelectron spectra were acquired with a Leybold LHS 10 spectrometer working in the $\Delta E$ = constant mode at a pass energy of 20 eV. The spectrometer was equipped with a magnesium anode X-ray excitation source ($MgK\alpha$ = 1253.6 eV) operated at 12 kV and 10 mA. The powdered extrudates were mounted on small stainless-steel holders on a standard long rod placed in an introduction chamber and outgassed at $10^{-5}$ Torr before being moved into the turbopumped analysis chamber. The pressure in this chamber was maintained below $3 \times 10^{-9}$ Torr during data acquisition. Several 20-eV energy regions of the photoelectrons of interest were scanned. Each spectral region was signal averaged for a number of scans in order to obtain satisfactory signal-to-noise ratios. Although surface charging was observed in all samples, accurate binding energies (BE) could

be determined by charge referencing with $C_{1s}$ peak at 284.6 eV.

*Infrared spectroscopy (FTIR).* Infrared experiments were carried out in a special cell assembled with greaseless stopcocks and KBr windows, which permitted either static or dynamic treatments. The powdered extrudates, were pressed into very thin wafers (thickness: 10.0–11.6 mg $cm^{-2}$). These samples were heated at 500°C, outgassed for 1 h, contacted with 100 Torr $H_2$ for 1 h, and then outgassed for 0.5 h. After cooling to room temperature, these were contacted with 35 Torr NO for 0.5 h and then the spectra were recorded on a Nicolet ZDXFTIR spectrophotometer at a resolution of 2 $cm^{-1}$.

*Optical microscope observation.* The optical microscope (Olympus Laboratory Microscope) was used for a preliminary definition of the type and the thickness of Mo macrodistributions. The extrudates studied were first immersed in an aqueous hydrazine–hydrochloric acid solution for 0.5 h. Next, the extrudates were cut into halves with a stainless razor blade, in order to expose their cross section. A well defined blue colour was found to be present in the extrudate regions where molybdenum oxide was deposited and leaching of molybdenum to the external solution did not occur.

*Specific surface area measurements (SSA).* The SSA of the catalysts were determined using a well known flow technique. This technique involves the uptake of an adsorbate from a flowing mixture of the adsorbate in an inert gas. Pure nitrogen (Linde special) and helium (Linde 99.996%) were used as adsorbate and inert gas, respectively, in a laboratory-constructed apparatus. The amount of nitrogen adsorbed at liquid-nitrogen temperature and at three different partial pressures was determined using a thermal conductivity detector of a gas chromatograph (Varian Series 1700).

*Temperature programmed reduction (TPR).* The TPR experiments were performed using a laboratory constructed equipment in which the ideas of the Rogers–Amenomiya–Robertson arrangement (*6*) have been followed. A weighed quantity of powdered extrudate (0.05 g) was placed in a quartz reactor and the reducing gas mixture ($H_2$/Ar : 5/95 v/v) was passed through it for 2 h with a flow rate of 40 ml $min^{-1}$ at room temperature. Next, the temperature was increased to 900°C at a constant rate of 12°C $min^{-1}$. Reduction led to a decrease of the hydrogen concentration in the gas mixture, detected by a thermal conductivity detector. The reducing gas mixture was dried in a cold trap (ca. −95°C) before reaching the catharometer.

### *Activity and Selectivity Measurements*

The catalytic tests were performed in a differential fixed bed reactor operating under atmospheric pressure. The hydrodesulfurization of thiophene (hds) and the hydrogenation of the produced olefins (hyd) were used as probe reactions. The catalysts in the form of extrudate or powder (one extrudate or one crushed extrudate) were presulfided in situ as follows: the reactor temperature was increased up to 400°C at a rate of 10°C $min^{-1}$ under argon stream. Next, a mixture of $H_2S/H_2$ (15/85 v/v) was fed for 2 h with a flow rate of 20 ml $min^{-1}$. The amount of the adsorbed $H_2S$ remaining after sulfidation was removed by flushing the sample with argon for 1 h at the same temperature. The reactor was next fed with the reaction mixture prepared by passing hydrogen through a simple flow evaporator filled with liquid thiophene at 0°C. The temperature was lowered to 250°C. After an aging period of 12 h under the reaction mixture stream, the conversion of thiophene, $X_t$, and the relative yield of butane, $Y_b$, were determined at 300, 325, and 350°C. A gas chromatograph (Pye Umicam) equipped with a flame ionization detector, a Chromosil 310 column (Supelco), and an integrator–recorder (Shimadzu C-RGA) was used to analyse the effluent of the reactor.

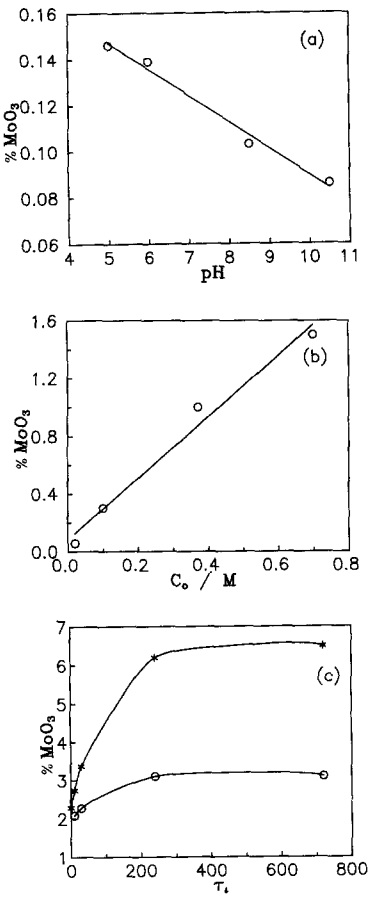


FIG. 1. Variation of the amount of $Mo^{(VI)}$ deposited on the support surface with the most important impregnation parameters: (a) variation with pH; (b) Variation with the initial $Mo^{(VI)}$ concentration of the impregnating solution; (c) Variation with impregnation time. (○, $C_0 = 0.02\ M$; *, $C_0 = 0.7\ M$).

## RESULTS AND DISCUSSION

### AXIAL PROFILES

#### *Amount of $Mo^{(VI)}$ Species Deposited on the γ-Alumina Surface*

Figure 1 illustrates the variation of the amount of $Mo^{(VI)}$ deposited on the support surface with the most important impregnation parameters, i.e., pH, concentration, and impregnation time. It may be seen that an increase in the $Mo^{(VI)}$ concentration of the impregnating solution and a decrease in its pH caused an increase in the amount of the deposited $Mo^{(VI)}$. It should be noted that an increase of the $Mo^{(VI)}$ concentration above a critical value caused undesired precipitation of $Mo^{(VI)}$ species in the solution. It is well known (*7–9*) that the concentration of the $AlOH_2^+$ surface groups increases at pH values lower than the pzc which was found to be at pH 5.3. The $AlOH_2^+$ groups are suggested to be the adsorption sites for the $Mo^{(VI)}$ species (*10–12*). At low pH values, therefore, it is anticipated that the $Mo^{(VI)}$ deposited shall be higher, as confirmed by the results shown in Fig. 1a. Concerning the influence of the impregnating time, it may be noted that a considerable increase in the $Mo^{(VI)}$ loading may be obtained by increasing the $\tau_i$ value from zero to 240. Further increase of the impregnating time did not have any appreciable effect on the $Mo^{(VI)}$ loading. It should be mentioned that the values of pH, $C_{Mo}$ and $\tau_i$ resulting to high (low) $Mo^{(VI)}$ loading favoured the formation of egg-shell (uniform) profile (*1*). It is therefore necessary to develop alternative methods, for instance, successive impregnations, if uniform profiles with high Mo loading are needed.

#### *Preparation of Egg-Shell and Egg-White Profiles*

In Fig. 2 the achievement of egg-white profiles from an egg-shell profile by successive pore volume impregnations with $NH_4OH$ may be seen. Ten (10) $NH_4OH$ impregnations were needed for an acceptable egg-white profile (Fig. 2, curve (c)). This method, therefore, is rather difficult to be suggested for industrial-scale application. The short impregnation time selected (see Fig. 1c) resulted in relatively low $Mo^{(VI)}$ loading in the initial profile (Fig. 2, curve (a)) and thus to low $Mo^{(VI)}$ loading (1.3% $MoO_3$) in the final egg-white profile (Fig. 2, curve (c)), despite the fact that the values selected for pH and solution concentration favoured relatively high $Mo^{(VI)}$ loading (see Figs. 1a and 1b). These findings were taken into consideration in the next preparation of egg-white profiles from an egg-shell profile.

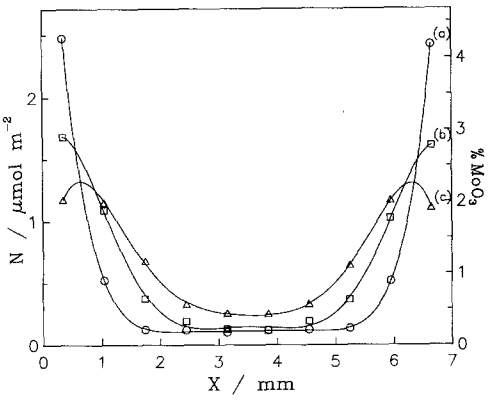


FIG. 2. Achievement of egg-white profiles from an egg-shell profile by successive pore volume impregnations with 0.1 *N* $NH_4OH$: (a) egg-shell profile ($C_{Mo}$ = 0.7 *M*, pH = 4.5, *T* = 25°C, $\tau_i$ = 10, Mo loading = 1.3% $MoO_3$); (b) four successive impregnations; (c) 10 successive impregnations (Mo loading = 1.3% $MoO_3$).

The results are illustrated in Fig. 3. It may be seen that a simple nondry $NH_4OH$ impregnation of extrudates, on which an egg-shell profile had been achieved (Fig. 3, curve (a)), was sufficient for obtaining an egg-white distribution. Moreover, it may be noted that the desorption time is a critical

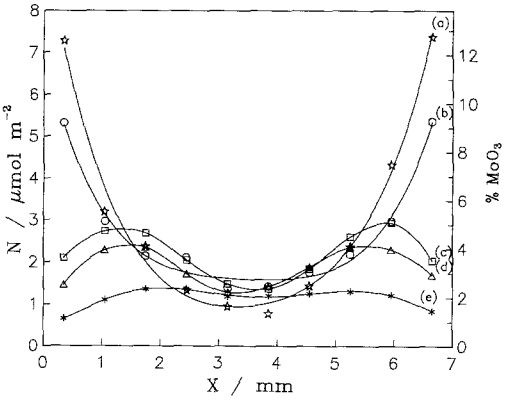


FIG. 3. Achievement of egg-white profiles from an egg-shell profile by simple non-dry impregnation with 0.1 *N* $NH_4OH$: (a) egg-shell profile ($C_{Mo}$ = 0.7 *M*, pH = 4.5, $\tau_i$ = 240, *T* = 25°C, $V_{Solution}/V_{pores}$ = 20, Mo loading = 6.2 %$MoO_3$); (b) $\tau_d$ = 10 (Mo loading = 5.5 %$MoO_3$); (c) $\tau_d$ = 50 (Mo loading = 3.9 %$MoO_3$); (d) $\tau_d$ = 80 (Mo loading = 3.4 %$MoO_3$); (e) $\tau_d$ = 120 (Mo loading = 2.0 %$MoO_3$).

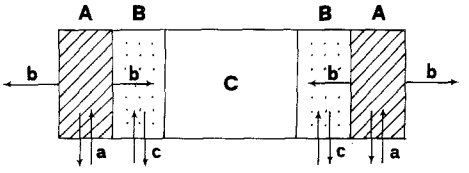


FIG. 4. Schematic representation of the mechanism of formation of an egg-white profile from an egg-shell profile: (a) desorption, (b) diffusion of the desorbed $MoO_4^{2-}$ ions, (c) readsorption.

parameter. In fact, for $\tau_d$ = 50, a fine egg-white profile was obtained (Fig. 3, curve (c)). Further increase in the desorption time caused a progressive transformation of the egg-white into an almost uniform profile (compare Fig. 3, curve (c) with curves (d) and (e)). Finally, it should be noted that the increase in the impregnation time from $\tau_i$ = 10 to $\tau_i$ = 240 allowed for the deposition of quite large amount of $Mo^{(VI)}$ on the support surface in the initial egg-shell profile (6.2% $MoO_3$ curve (a) in Fig. 3) and therefore, in the final egg-white profile (3.9% $MoO_3$ in curve (c), Fig. 3).

Next, it should be attempted to explain the fact that the desorption of the $Mo^{(VI)}$ species from the support surface, taking place during the dry or nondry impregnation with $NH_4OH$, caused the transformation of an egg-shell into an egg-white profile. As may be seen in Fig. 4 (regions A) the rate of desorption of $Mo^{(VI)}$ species should be much higher at the outer regions than the interior of the extrudates.

Taking into account the initial egg-shell profiles (Fig. 2 and 3), it may be suggested that all of the $Mo^{(VI)}$ species were practically desorbed from the outer regions of the extrudates. The molybdenum species, which in alkaline pH values are predominantly $MoO_4^{2-}$ ions (*9–11*), should diffuse through the liquid phase into regions with lower $Mo^{(VI)}$ concentration. Such regions are the external solution and the interior of the extrudates. The molybdates in the interior are readsorbed on the $\gamma$-alumina surface, mainly on regions very close to the outer

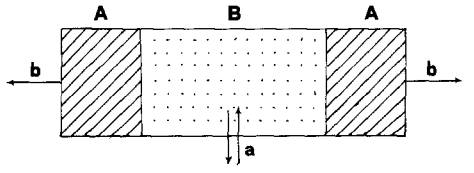


FIG. 5. Schematic representation of the mechanism of formation of an egg-yolk profile from a uniform profile: (a) desorption, (b) diffusion of the desorbed $MoO_4^{2-}$ ions to the external solution.

regions of the extrudates (regions B, Fig. 4), thus yielding an egg-white profile. Considering that the concentration of the external solution for $\tau_d = 0$ is equal to zero, the initial rate of diffusion towards the external solution is considerably higher than the rate towards the interior of the extrudate. For this reason, the first result of the impregnation with $NH_4OH$ is simply the decrease in the Mo loading in the A regions of the extrudates (compare curve (a) with curve (b) in Fig. 3). The rate of diffusion towards the external solution decreased with increasing time, whereas more $MoO_4^{2-}$ ions diffused and were readsorbed on the regions B, causing the formation of an egg-white profile (Fig. 3, curve (c)). Further increase in the desorption time allowed for the $MoO_4^{-2}$ to diffuse and be readsorbed in the region C (Fig. 4), thus causing a progressive transformation of the egg-white into a uniform profile (Fig. 3, curve (e)).

In the case of dry impregnation with $NH_4OH$ solution it may be argued that a similar qualitative model is valid with the only difference that there is no diffusion outside the extrudate. In order to explain why a rather large number of dry impregnations was required for obtaining an egg-white profile, the pH variation of the impregnating solution inside the pores should be taken into account. In fact, as the point of zero charge of both alumina (5.3) and molybdenum oxide (2.6) (*13*) are lower than the pH of the $NH_4OH$ solution, the latter decreased as the solution penetrated the pores of the extrudates (*14–16*). In such a case the rate of desorption of molybdenum–oxo species is very low. Past a number of successive impregnations with the $NH_4OH$ solution the catalyst surface groups (–OH) in the outer part of the extrudate (region A) were fully deprotonated and thus no pH change occurred, which would lead to an increase of the desorption rate. In Fig. 2, curve (c) it may be seen that 10 successive impregnations with $NH_4OH$ aqueous solutions were required in order for a considerable decrease of the Mo loading in the A regions to be achieved.

### *Preparation of Uniform and Egg-Yolk Profiles*

Taking into account the model described above, we attempted to tailor the preparation of an egg-yolk profile. We started with a uniform profile and we tried to remove, by impregnating with $NH_4OH$ solution, the deposited $Mo^{(VI)}$ from the region A of the extrudates (Fig. 5). According to the forementioned model, two steps are involved: (i) desorption of the supported $Mo^{(VI)}$ species and (ii) diffusion of the $MoO_4^{2-}$ ions from the extrudate into the bulk solution. Due to the fact that the initial Mo loading is almost constant over the entire extrudate, the rate of desorption should be the same in all parts of the extrudates. However, taking into account the pH change of $NH_4OH$ solution as it penetrated in the pores of extrudates, it may be suggested that a pH gradient was developed decreasing from the outer part to the interior of the extrudate. This pH gradient resulted in higher desorption and removal rates of $Mo^{(VI)}$ species from the outer part (region A) than from the interior (region B) of the extrudates. For an appropriate desorption time, therefore the formation of an egg-yolk profile from a uniform profile may be anticipated. The results shown in Fig. 6 confirmed our predictions. For $\tau_d$ values in the range 30–80 egg-yolk profiles have been obtained. It may be seen that up to a critical value of $\tau_d$ the width of the egg-yolk profile decreased with increasing desorption time in accordance with the

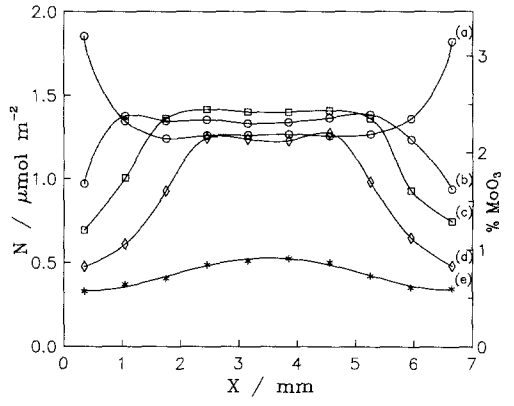


FIG. 6. Achievement of egg-yolk profiles from a uniform profile by simple non-dry impregnation with 0.1 $N$ $NH_4OH$: (a) uniform profile ($C_{Mo}$ : 0.7 $M$, pH = 10, $\tau_i$ = 240, $T$ = 25°C $V_{solution}/V_{pores}$ = 20, Mo loading = 3.1 %$MoO_3$) (b) $\tau_d$ = 30 (Mo loading = 2.1 %$MoO_3$) (c) $\tau_d$ = 50 (Mo loading = 1.9 %$MoO_3$) (d) $\tau_d$ = 80 (Mo loading = 1.5 %$MoO_3$) (e) $\tau_d$ = 120 (Mo loading = 0.74 %$MoO_3$).

model proposed. However, further increase of the desorption time, leading to elimination of the pH gradient, resulted in the removal of the $Mo^{(VI)}$ deposited even in the interior of the extrudates and yielded a uniform profile with very low Mo loading (Fig. 6, curve (e)).

The experimental results so far show that the desorption time is a critical parameter. According to the model proposed the values of $\tau_d$ used in order for obtaining an egg-yolk profile should depend on the desorption rate. Increase of the desorption rate is expected to cause an increase of the $Mo^{(VI)}$ concentration in the liquid phase within the extrudate, and consequently an increase in the diffusion rate to the bulk solution. The two rates become equal at the steady state. It was therefore anticipated that at desorption times where an egg-yolk profile was obtained, a uniform profile should be obtained by increasing the rate of desorption. Two experiments have been done in order to study the effect of the rate of desorption. First, we impregnated extrudates with a uniform profile with a concentrated (7 $N$) $NH_4OH$ aqueous solution. Second, we impregnated these extrudates with 0.1 $N$ $NH_4OH$, but this time without drying after the impregnation step with AHM needed to obtain the initial uniform Mo profile. The results illustrated in Fig. 7(a,b,c) confirmed our predictions; instead of an egg-yolk profile, a uniform profile with low $Mo^{(VI)}$ loading was obtained in both cases. The experimental results have clearly shown that the stabilisation of the supported Mo before impregnating with $NH_4OH$, the concentration of

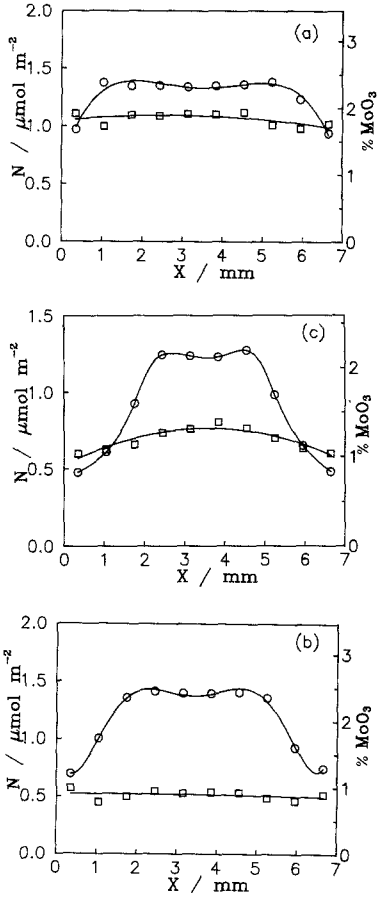


FIG. 7. Influence of the concentration of the $NH_4OH$ aqueous solution and of drying on the Mo profile achieved. (a) Influence of the $NH_4OH$ concentration: □, 7 $N$ $NH_4OH$, $\tau_d$ = 30; ○, 0.1 $N$ $NH_4OH$, $\tau_d$ = 30. (b) Influence of drying before desorption: ○, $\tau_d$ = 50 dried; □, $\tau_d$ = 50 nondried extrudates. (c) Influence of drying after desorption: ○, drying at 120°C for 2 h; □, drying at 25°C for 20 h.

the $NH_4OH$ solution as well as the desorption time should be carefully regulated in order for an egg-yolk profile to be achieved. Concerning the latter parameter, it should be noted that desorption, diffusion, and readsorption continued during the step of drying after the impregnation with $NH_4OH$. Prolonged drying at relatively low temperature favouring the formation of uniform profiles (Fig. 7c) should therefore be avoided.

*General Remarks*

Careful examination of the experimental results plotted in Figs. 2, 3, and 6 showed that the methods established may result in egg-white and egg-yolk profiles from egg-shell and uniform profiles, respectively, but the $Mo^{(VI)}$ loading obtained is rather low. This is particularly true for the uniform and egg-yolk profiles. As already mentioned, the proper regulation of the impregnation parameters resulted to some increase of the final $Mo^{(VI)}$ loading but in the cases where higher $Mo^{(VI)}$ loading is required, the application of successive AHM impregnations followed by drying seems to be inevitable.

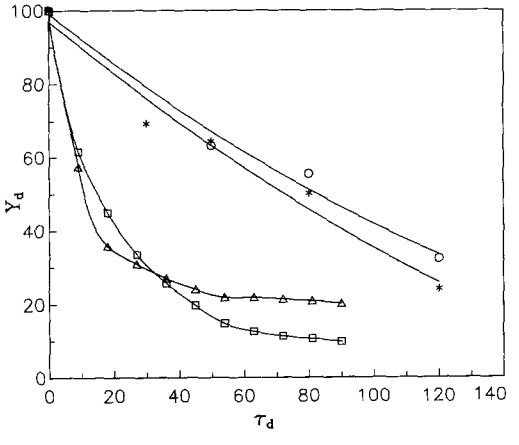


FIG. 8. Kinetics of desorption of $Mo^{(VI)}$ species during impregnation with 0.1 *N* $NH_4OH$ aqueous solution related with the achievement of egg-white and egg-yolk profiles from egg-shell and uniform profiles, respectively. ($Y_d$ = ([$\mu$moles Mo/g]$_{\tau d=0}$/[$\mu$moles Mo/g]$_{\tau d}$) × 100.) ○, egg-shell → egg-white (axial); *, uniform → egg-yolk (axial); △, egg-shell → egg-white (radial); □, uniform → egg-yolk (radial).

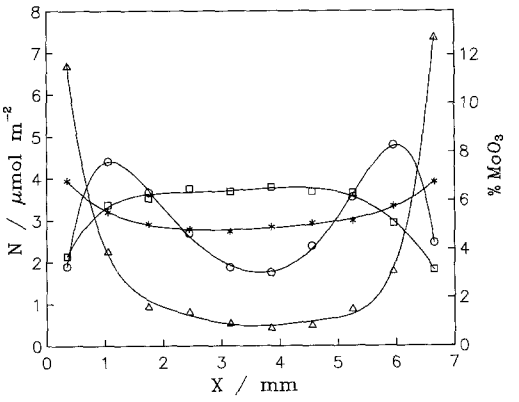


FIG. 9. Typical examples of the prepared $MoO_3/\gamma$-$Al_2O_3$ axial profiles: △, egg-shell profile ($C_{Mo}$ = 0.9 *M*, pH = 4.5, $\tau_i$ = 1, *T* = 25°C, drying at 120°C for 2 h, Mo loading = 5.2% $MoO_3$); *, uniform profile ($C_{Mo}$ = 1 *M*, pH = 10, $\tau_i$ = 1, *T* = 25°C, drying at 25°C for 20 h and then at 120°C for 2 h, Mo loading = 5.6% $MoO_3$); ○, egg-white profile ($C_{Mo}$ = 1.5 *M*, pH = 5.5, $\tau_i$ = 1, drying at 120°C for 2 h, $\tau_d$ = 60, drying after desorption at 120°C for 2 h, Mo loading = 5.3% $MoO_3$); □, egg-yolk profile ($C_{Mo}$ = 1.25 *M*, pH = 10, $\tau_i$ = 1, drying at 25°C for 20 h, and then at 120°C for 2 h, $\tau_d$ = 60, drying after desorption at 120°C for 2 h, Mo loading = 14% $MoO_3$).

A further task of the present work was the achievement of the four Mo macrodistributions described here with equal $Mo^{(VI)}$ loading. This was necessary, since the relationship between the type of the profile achieved and the catalytic properties should be further investigated. For this purpose, it is important to know not only the $Mo^{(VI)}$ loading in the initial egg-shell or uniform profiles, but also the amount of the $Mo^{(VI)}$ left on the support surface after a given desorption time. To this end, the results illustrated in Fig. 8 showing the dependence of the percentage of the mount desorbed, $Y_d$, on the desorption time, $\tau_d$, are apparently very useful. Concerning the axial profiles, it may be noted that the "rate" of the $Mo^{(VI)}$ removal was slightly higher for the $Mo^{(VI)}$ desorbed from the egg-shell than from the uniform profile, as was anticipated. These results were used for the preparation of $Mo^{(VI)}/\gamma$-$Al_2O_3$ catalysts with almost the same $Mo^{(VI)}$ loading in all Mo profiles. A typical example is shown in Fig. 9.

## Radial Profiles

### *Preparation*

As already mentioned for egg-shell and uniform macrodistributions, it was found that similar axial and radial profiles were obtained under the same experimental conditions (*1*).

It is, therefore, reasonable to investigate whether the impregnation with $NH_4OH$ used in the case of axial profiles for the preparation of egg-white (egg-yolk) profiles from egg-shell (uniform) profiles may be also applied for radial profiles. This issue was investigated through the experiments described in the "Kinetics of Desorption of Supported $Mo^{(VI)}$ species" of the experimental part. These experiments allowed us to observe, using an optical microscope, the changes on an egg-shell or uniform radial profiles as the desorption time increased. As in the case of axial profiles, it was found that as the desorption time increased a uniform profile was progressively transformed into an egg-yolk profile (Fig. 10). For the same reasons, an egg-shell profile was merged into an egg-white one. Moreover, these experiments allowed the determination of the amount of the $Mo^{(VI)}$ left on the support surface past a certain desorption time. As already mentioned, for axial profiles this parameter was necessary in order to design the preparation of egg-white and egg-yolk radial profiles with a desired $Mo^{(VI)}$ loading. Figure 8 shows that the "rate" of $Mo^{(VI)}$ removal was higher for radial than axial profiles. This finding was expected, because the surface area from where the $MoO_4^{2-}$ ions diffused into the bulk solution is $2\pi r^2 + 2\pi rl$ for radial and $2\pi r^2$ for axial profiles ($r$ and $l$ represent the radius and the length of the extrudate, respectively).

The experience accumulated during our work on axial profiles, as well as our preliminary results on radial profiles presented above, proved to be very useful in establishing the procedure and in determining the conditions for the preparation of all types of Mo radial profiles. Following the procedure described in the experimental part, we were able to prepare the four Mo radial profiles with the desired, almost the same, $Mo^{(VI)}$ loading, (Figs. 11a to d). A loading of 12–14% $MoO_3$, typically encountered in the industrial Mo-supported hydrodesulfurization catalysts, was chosen.

It should be mentioned that a simple impregnation was sufficient in order for an amount of $Mo^{(VI)}$ corresponding to 13.1% $MoO_3$ to be deposited in the case of the uniform profile. This occurred because the alkaline pH of the solution (pH = 10) made it possible for the deposition to be done from a very concentrated but stable solution ($C_{Mo}$ = 1.13 *M*). In contrast to that, the low pH did not allow the preparation of a very concentrated $Mo^{(VI)}$ solution in the case of the egg-shell profile. A double successive impregnation was therefore necessary in order to deposit a quantity corresponding to 12% $MoO_3$. Finally, the fact that a portion of the supported Mo was removed during $NH_4OH$ impregnation imposed the need for three successive impregnations for the preparation of the egg-white and egg-yolk profiles.

### *Characterization*

In the following, we discuss the results of physicochemical characterization of the

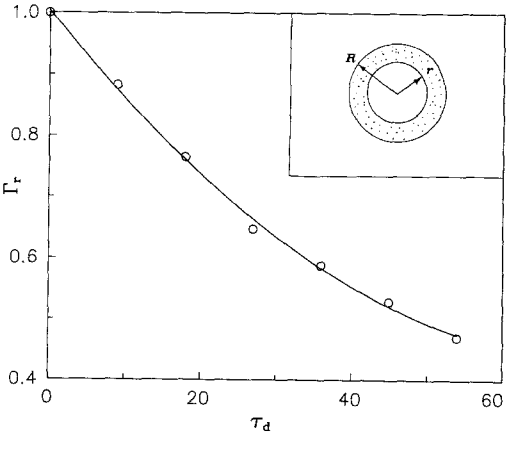


FIG. 10. Progressive transformation of a uniform profile into egg-yolk after impregnation with $NH_4OH$ solution radially.

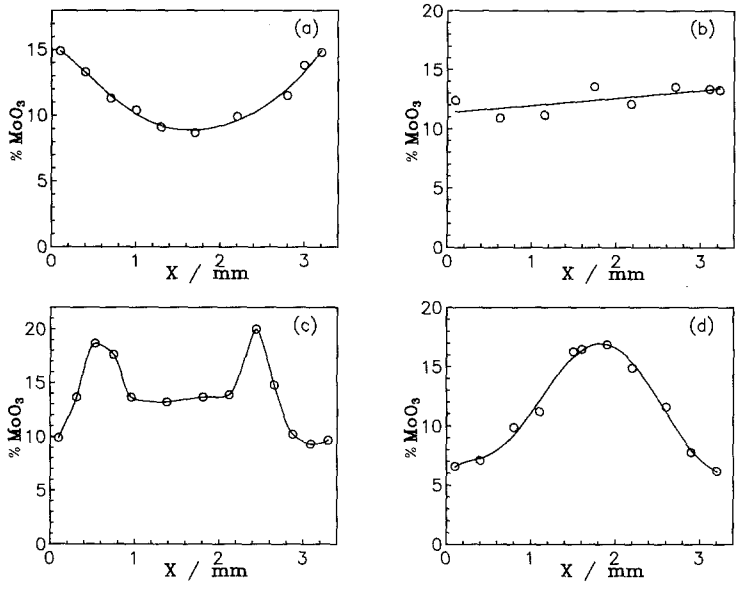


FIG. 11. Radial Mo/γ-alumina profiles achieved in the present work: (a) egg-shell profile [$C_{Mo}$ = 0.74 $M$, pH = 4.5, $\tau_i$ = 10 (two successive impregnations), drying at 120°C for 2 h and calcination at 300°C for 1 h, and then at 550°C for 5 h, Mo loading = 12% $MoO_3$]; (b) uniform profile [$C_{Mo}$ = 1.13 $M$, pH = 10, $\tau_i$ = 10 (simple impregnation), drying at 25°C for 20 h and then at 120°C for 2 h, calcination at 300°C for 1 h and then at 550°C for 5h, Mo loading = 13% $MoO_3$); (c) egg-white profile [$C_{Mo}$ = 0.82 $M$, pH = 5.5, $\tau_i$ = 10 (three successive impregnations), drying before desorption at 120°C for 2 h, $\tau_d$ = 90, drying after desorption at 120°C for 2 h, calcination, Mo loading = 13.7% $MoO_3$]; (d) egg-yolk profile [$C_{Mo}$ = 1.25 $M$, pH = 10, $\tau_i$ = 10 (three successive impregnations), drying before desorption at 25°C for 20 h and then at 120°C for 2 h, impregnation for $\tau_d$ = 246, drying after each desorption at 120°C for 2 h, calcination, Mo loading = 14% $MoO_3$].

radial profiles prepared. As was stated in the experimental part of this article, the characterization done was performed on oxidic (XPS, TPR, BET) and reduced (NO adsorption) state, whereas the catalytic tests were performed in the sulfided state. Taking into account that Mo dispersion is different in the reduced and sulfided state as compared with that in the oxidic one, the above approach could create some questions. However, one cannot expect that the reduction or sulfidation should change the trends related to the dispersity or active sites population.

The X-ray photoelectron spectra of the $Mo^{(VI)}$ 3*d* photoelectrons recorded for the radial profiles prepared are illustrated in Fig. 12. In all cases the typical doublet, with binding energies at about 233.3 eV (Mo3*d* 5/2) and 236.3 eV (Mo3*d* 3/2) may be seen indicating the presence of the supported $Mo^{(VI)}$(*17–20*). Careful examination of the spectra showed that the binding energies in the case of the egg-shell profile were higher compared to those of the other profiles. This is a strong indication that the "$Mo^{(VI)}$ supported species–support" interactions are relatively strong in the egg-shell profile. In order to explain this observation we should consider that the deposition of the $Mo^{(VI)}$ ions on the γ-alumina surface may be effected through the following processes: (i) adsorption of the $Mo^{(VI)}$ species during impregnation and (ii) precipitation of these species during the step of drying. The ratio of the adsorbed to the precipitated $Mo^{(VI)}$, $Mo_a^{(VI)}/Mo_p^{(VI)}$, depends on the value of the impregnation parameters, mainly on pH and

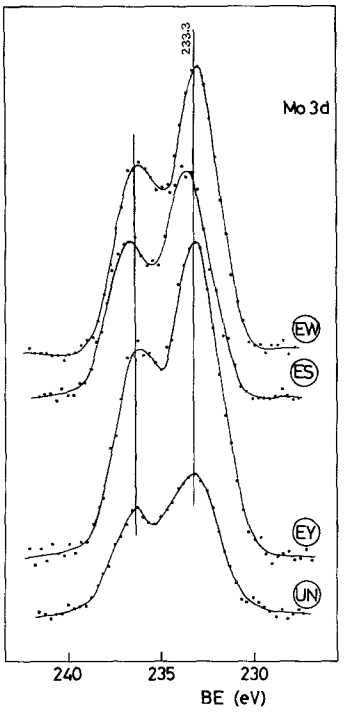


FIG. 12. XPS spectra of the $Mo_{3d}^{(VI)}$ photoelectrons for the Mo/γ-alumina radial profiles achieved.

concentration of the impregnating solution. Low pH is related with relatively high density of adsorption sites (*10–12*), whereas low $Mo^{(VI)}$ concentration does not favour precipitation. These conditions, encountered in the preparation of the egg-shell profile, resulted in the increase of the $Mo_a^{(VI)}/Mo_p^{(VI)}$ ratio, and thus of the $Mo^{(VI)}$ amount which interacted strongly with the support surface. Extrapolation of the above explanation to the other profiles suggested the following classification of the profiles in the order of increasing "supported Mo-support" interactions: egg-shell ($pH_i$ = 4.5, $C_{Mo}$ = 0.74 *M*) > egg-white ($pH_i$ = 5.5, $C_{Mo}$ = 0.82 *M*, $pH_d$ = 10) > uniform ($pH_i$ = 10, $C_{Mo}$ = 1.13 *M*) > egg-yolk($pH_i$ = 10, $C_{Mo}$ = 1.25 *M*, $pH_d$ = 10).

The temperature programmed reduction curves, presented in Fig. 13, corroborated the above assumption. In agreement with the literature, two peaks appeared in these curves (*21, 22*). The first, centered at about 550°C, was attributed to the reduction of the supported $Mo^{(VI)}$ being in the supported double layer whereas the second, centered at about 850°C, was attributed to the reduction of the supported $Mo^{(VI)}$ monolayer, which interacted mainly with the support (*23–26*). A progressive shift of the second peak to higher reduction temperatures from the egg-yolk to the egg-shell profiles indicated a corresponding progressive increase in the "supported $Mo^{(VI)}$-support" interactions, thus confirming the order assumed above. With the exception of the egg-white profile a similar shift of the first reduction peak may be observed. In conclusion, the XPS but mainly the TPR results suggested a progressive increase of the "Mo supported-support" interactions from the egg-yolk to the egg-shell profile (*27, 28*).

It is well known that deposition by adsorption results to better dispersion of the supported ions compared to the deposition taking place by precipitation (*13*). It is therefore anticipated that the increase of the $Mo_a^{(VI)}/Mo_p^{(VI)}$ ratio from the egg-yolk to egg-shell profile assumed above should also cause an analogous increase in the dispersion of the supported $Mo^{(VI)}$. This prediction was indeed confirmed by the XPS measurements (Table 1).

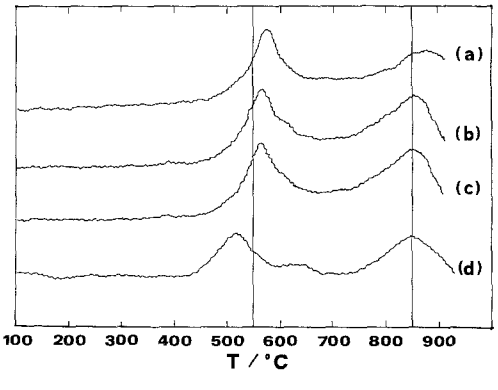


FIG. 13. TPR curves of the Mo/γ-alumina radial profiles achieved in the present work: (a) egg-shell profile, (b) egg-white profile, (c) uniform profile, (d) egg-yolk profile.

TABLE 1

Mo Content, Specific Surface Area (SSA), Dispersion ($D$), and Values of IANB[a] for the Radial Profiles Prepared

| Catalyst | %$MoO_3$ | SSA | $D^b$ | IANB |
|---|---|---|---|---|
| Egg-shell | 12.0 | 114 | 13.440 | 12.000 |
| Egg-white | 13.7 | 117 | 12.273 | 10.206 |
| Uniform | 13.1 | 106 | 11.313 | 4.984 |
| Egg-yolk | 14.0 | 119 | 9.870 | 7.724 |
| $\gamma$-alumina | — | 120 | — | — |

[a] See text.

[b] It is determined by $D = (I_{Mo3d}/I_{Al3d}) * (_{NAl}/N_{Mo})$

The increase in the dispersion from the egg-yolk to the egg-shell profile is expected to have an influence on the number of active sites which can be estimated by NO adsorption. In Fig. 14 the FT-IR spectra of the adsorbed NO may be seen. Two bands appeared, centered at about 1815 and 1711 $cm^{-1}$, which indicated the presence of adsorbed NO (*29*). The integrated absorbance of the NO bands, (IANB), namely, the area under the bands, may be used for estimating the number of active sites (*30, 31*). The values of IANB compiled in the Table 1 show that the trend followed is similar but not identical with that followed for dispersion. The only difference was that the value of the IANB obtained for the egg-yolk profile was higher than that of the uniform profile. The opposite was true for dispersion. To explain this observation it is necessary to note that the number of active sites depends on two parameters: (i) on the Mo surface which is proportional to dispersion and (ii) on the density of the active sites, namely, on the number of active sites per unit $Mo^{(VI)}$ surface area. The second parameter is affected from the kind of the supported $Mo^{(VI)}$ species. According to the literature, the sites responsible for the NO chemisorption are the coordinatively unsaturated sites of sulphided/reduced Mo created from the tetrahedral $Mo^{(VI)}$ after sulfidation/or reduction (*32–36*). It was suggested that during the transformation for the uniform to egg-yolk profile, mainly the $Mo^{(VI)}$ supported octahedral species weakly bound on the support surface compared to the tetrahedral $Mo^{(VI)}$ species, were desorbed resulting to an increment of the ratio, tetrahedral $Mo^{(VI)}$/octahedral $Mo^{(VI)}$ and thus to the relatively large NO adsorption in the egg-yolk profile (*37*).

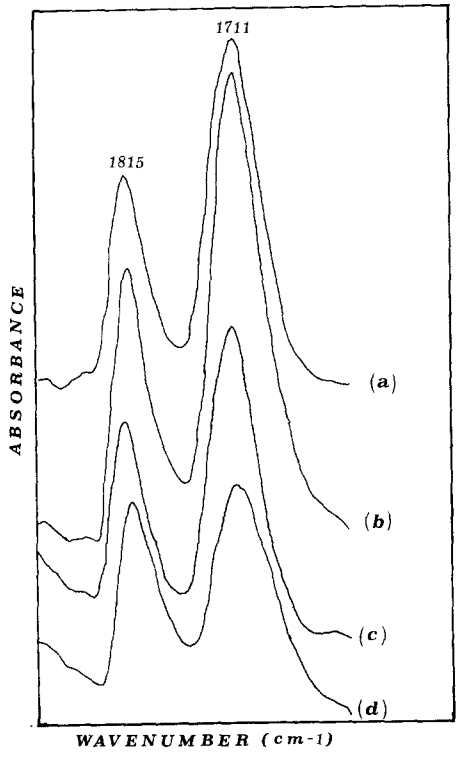


FIG. 14. FT-IR spectra of the adsorbed NO for the Mo/$\gamma$-alumina radial profiles achieved: (a) egg-white profile, (b) egg-shell profile, (c) egg-yolk profile, (d) uniform profile.

*Activity*

In Fig. 15 the rate of hds of thiophene, determined at three different temperatures, against Mo dispersion is plotted. The broken lines refer to the hds on extrudates, whereas the solid lines refer to the hds on powders produced by crushing the extrudates. The absence of any correlation clearly showed that the catalytic activity does not depend on this simple "geometrical" parameter. Contrary to that, with the exception of the egg-shell profile, a very good correlation

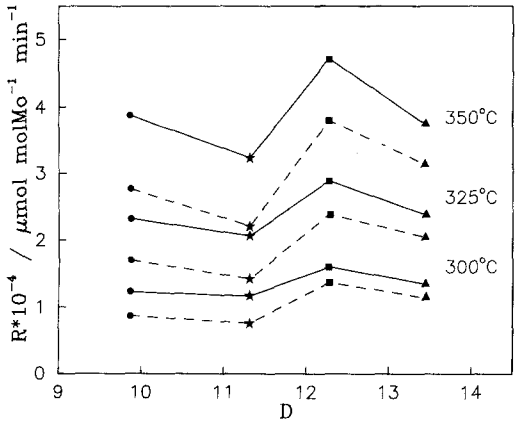


FIG. 15. Rate of hds of thiophene determined at various temperatures against Mo dispersion. The values of temperatures are indicated: (----) reaction on extrudates; (——) reaction on powdered extrudates; (●, egg-yolk; *, uniform; ■, egg-white; ▲, egg-shell.

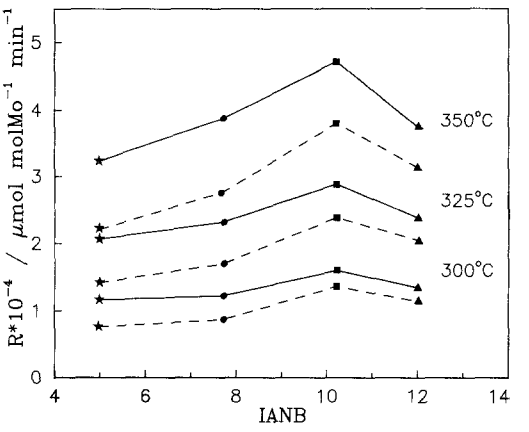


FIG. 16. Rate of hds of thiophene determined at various temperatures against IANB. The values of temperature are indicated: (----) reaction on extrudates; (——) reaction on powdered extrudates; *, uniform; ●, egg-yolk; ■, egg-white; ▲, egg-shell.

was found between the rate of hds and IANB. It may therefore be suggested that the catalytic activity increased with the number of active sites (Fig. 16). Concerning the egg-shell profile that the observed relatively low activity should be attributed to low activity per active site, fact which in turn should be related with the strong Mo–support interactions found by the TPR and XPS experiments (*38*).

Inspection of Figs. 15 and 16 showed that in all cases the rates measured with powders were higher than the measured with extrudates. This fact suggested the prevalence of diffusional effects. The magnitude however of these effects was not sufficient to cause changes in the trend of the observed activity in the powder catalysts. In other words, the hds activity of extrudates was mainly determined by the intrinsic activity, related to the number and quality of active centers, and not by the Mo macrodistribution achieved (*39*). The macrodistribution however, is expected to affect the magnitude of the diffusional effects. In Table 2 the values of the effectiveness factor, $\eta$, determined for the Mo profiles examined are summarized. Examination of the data shown in Table 2 showed that the observed trend $\eta_{\text{egg-shell}} > \eta_{\text{egg-white}} > \eta_{\text{egg-yolk}}$ was anticipated because the magnitude of the diffusional effects should increase as the maximum of the Mo profile shifted from the outer part to the center of the extrudate (*40*). However, the relatively low value obtained for the uniform profile was rather unexpected. In this case, it may be speculated that the preparation method followed, favouring deposition by precipitation, caused a partial clogging of the pores of the support. As a consequence the access of the reactant to the active material was hindered. This fact was corroborated by the value of SSA measured for the uniform distribution (Table 1), which was

TABLE 2

Values of the Effectiveness Factor, $\eta$, Determined for the hds of Thiophene over Mo Catalysts with Different Mo Profiles

| Catalyst | $\eta$ |
|---|---|
| Egg-shell | 0.848 |
| Egg-white | 0.829 |
| Uniform | 0.675 |
| Egg-yolk | 0.719 |

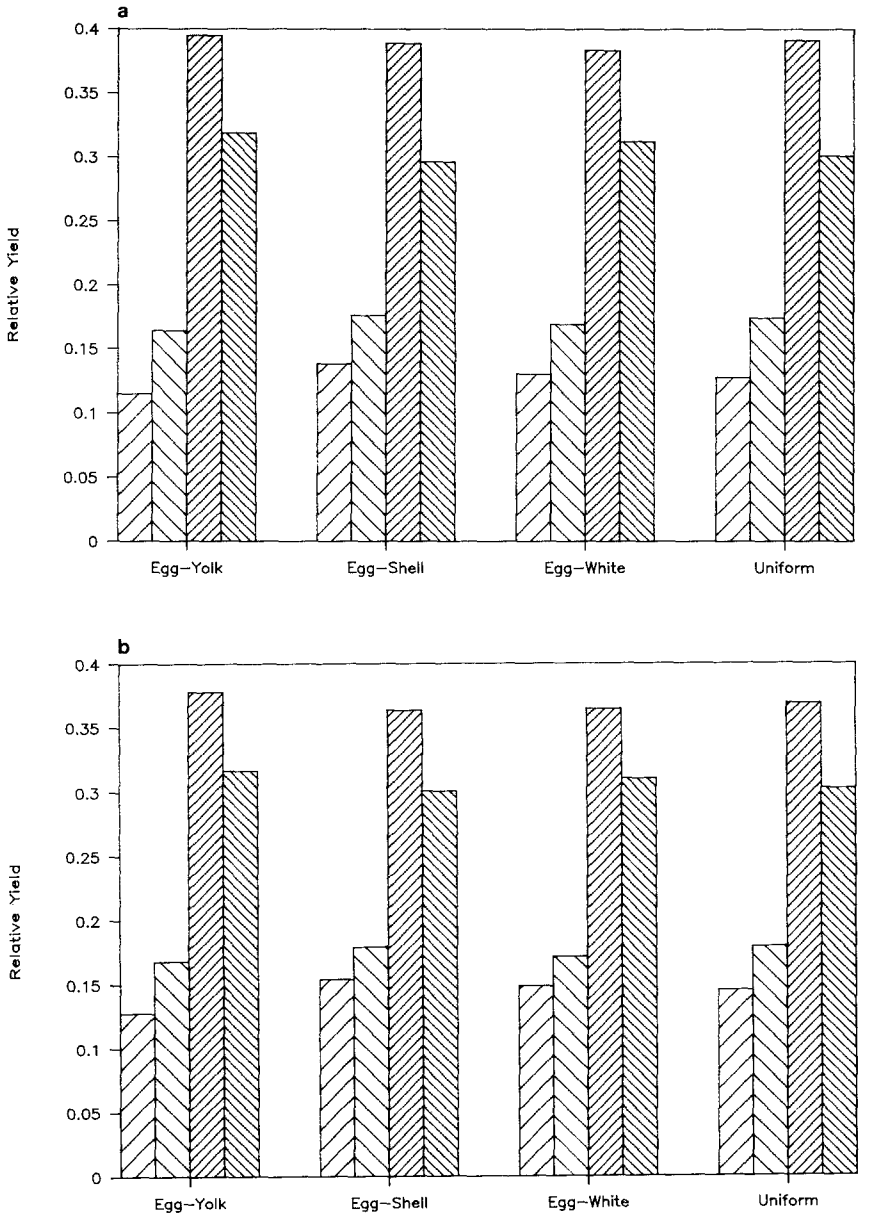


FIG. 17. Relative yields obtained for Pr1 = butane ▨, Pr2 = 1-butene ▧, Pr3 = *trans*-2-butene ▨, and Pr4 = *cis*-2-butene ▧ over powdered extrudates, at various temperatures: (a) 300°C, (b) 325°C, (c) 350°C. The type of the Mo profile is indicated.

found to be lower than the SSA values for the other macrodistributions.

*Selectivity*

Figure 17 illustrates the relative yields obtained for butane, 1-butene, *trans*-2-butene, and *cis*-2-butene in powdered extrudates at three different temperatures. It may be seen that at a given temperature the relative yields are constant irrespective of the Mo profile of extrudates from which the powder was produced. This showed clearly that the

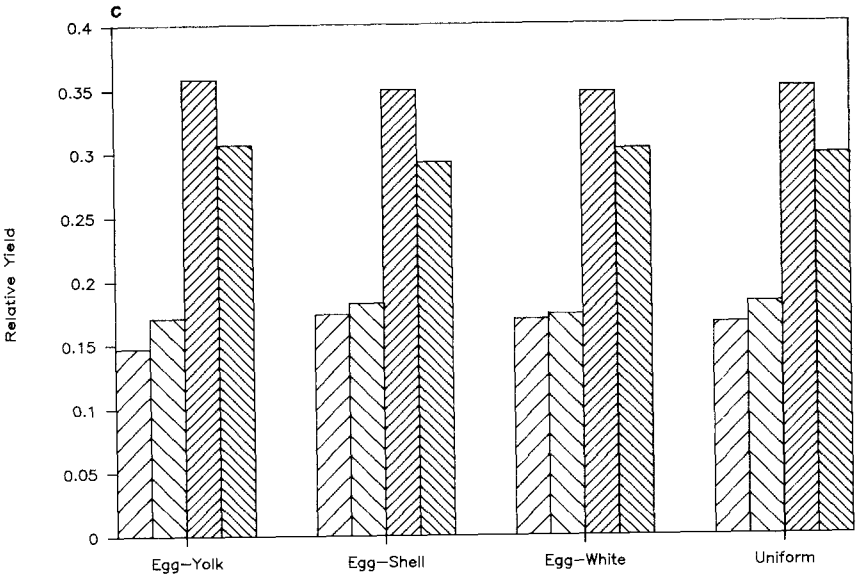


FIG. 17—*Continued*

differences in the relative yields achieved in extrudates at three different temperatures, (Fig. 18) should be attributed exclusively to the type of the Mo profile. Careful observation of this figure showed that the change in the relative field of butane was the most important. The trend observed, namely, $Y_{\text{egg-yolk}} > Y_{\text{egg-white}} > Y_{\text{egg-shell}} > Y_{\text{uniform}}$, should be explained. Taking into account that the relative yield of butane should be increased with the time that a molecule of an unsaturated hydrocarbon (produced by hds) remains inside the extrudate, the trend observed was rather expectable. In fact, in the first three profiles shown above, i.e., egg-yolk, egg-white, and egg-shell, the relative yield of butane increased with the distance of the maximum of the Mo profile from the periphery of the extrudate (Fig. 19), which was proportional to the molecules residence time in extrudate.

With respect to the uniform profile the suggestional partial clogging of the pores during the preparation process was consistent with the $\eta$ value obtained. Moreover, it may explain the low value of the relative yield because in this case the unsaturated hydrocarbons, produced mainly on the mouth of the pores and on the external surface, were relatively difficult to be hydrogenated before being desorbed from the catalyst surface.

Finally, it should be noted that the most active extrudates for hydrodesulfurization and hydrogenation were those where an egg-white and an egg-yolk Mo profile were achieved, respectively. The uniform profile exhibited the lowest activities for both reactions.

## CONCLUSIONS

The most important findings of the present study may be summarised as follows:

a. Concerning the axial Mo profiles on $\gamma$-alumina extrudates, it was confirmed that impregnation of these extrudates with AHM solution resulted to egg-shell and uniform profiles. The type of the profiles achieved depends on the selective value of the impregnating parameters (pH, temperature, impregnation time, concentration of the impregnating solution, . . .). A proper regulation of these parameters, mainly of the impregnation time, allowed us to deposit

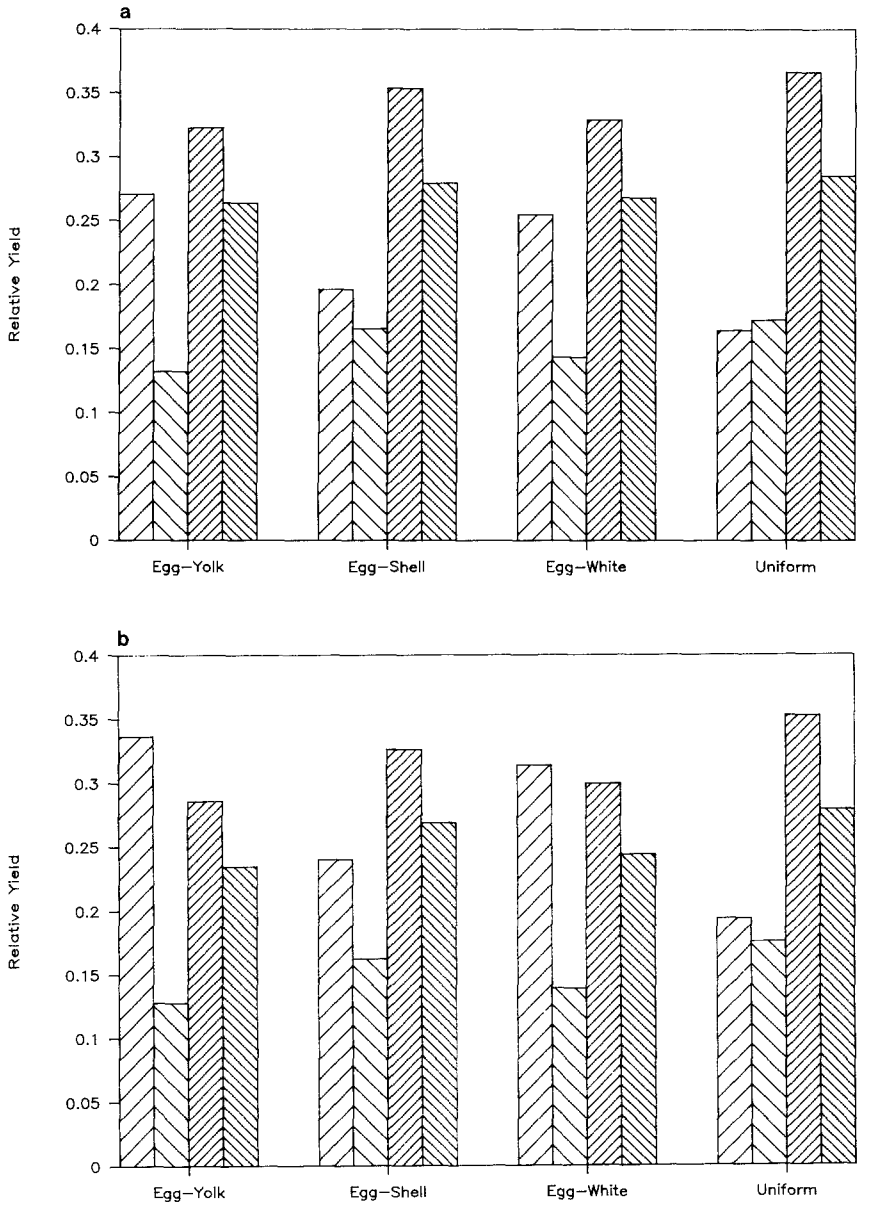


FIG. 18. Relative yields obtained for Pr1 = butane ▨, Pr2 = 1-butene ▧, Pr3 = *trans*-2-bytene ▨, Pr4 = *cis*-2-butene □ over pellet extrudates at various temperatures: (a) 300°C, (b) 325°C, (c) 350°C. The type of Mo profile is indicated.

relatively large amounts of Mo on the $\gamma$-alumina surface. Moreover, it was found that an egg-white (egg-yolk) profile may be achieved from an egg-shell (uniform) profile by successive pore volume or simple nondry impregnations of the estrudates with $NH_4OH$ aqueous solutions. During this impregnation, $MoO_4^{2-}$ ions were desorbed from the surface and were moved to the external solutions and to the interior of the

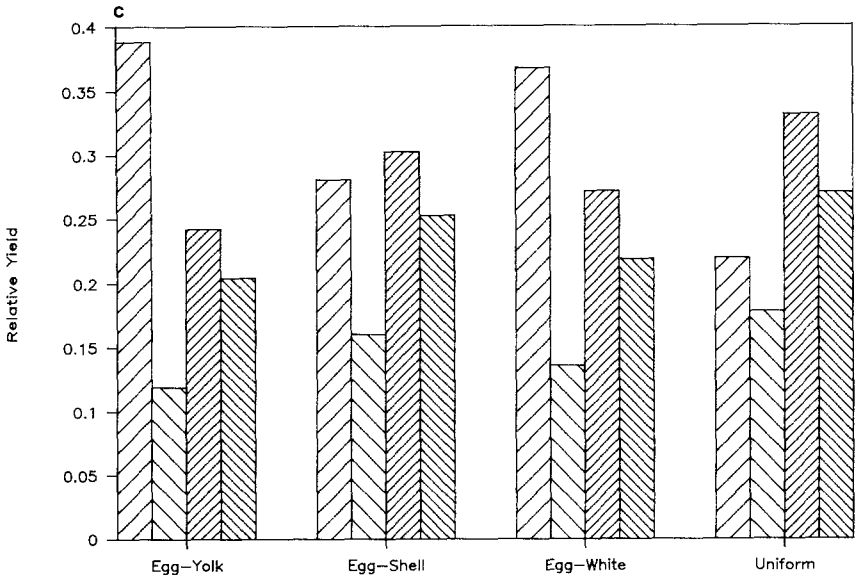


FIG. 18–*Continued*

extrudates where they were redeposited. A qualitative mechanism based on the relative rates of desorption and diffusion of the $MoO_4^{2-}$ ions was developed to interpret the influence of desorption time, concentration of the $NH_4OH$ solution, drying (before and after Mo desorption), and the type of impregnation (dry or non-dry) on the characteristics (e.g., width) of the egg-white and egg-yolk profiles achieved.

The above findings enabled us to prepare axially all types of the Mo profiles with almost the same, quite large, Mo content.

b. The application of the same procedure with that developed for the preparation of the Mo axial profiles as well as kinetic results on Mo desorption permitted the preparation of all types of Mo radial profiles with Mo content at the levels used in industrial applications.

c. Detailed characterization of Mo/$\gamma$-alumina powders, produced by crushing of extrudates on which the formentioned profiles were obtained, was done using XPS, TPR, BET, and FT-IR of adsorbed NO measurements.

The binding energies obtained for the $Mo_{3d3/2}$ and $Mo_{3d5/2}$ photoelectrons and the TPR curves obtained suggested a progressive increase of the "Mo supported–support" interactions following the order egg-yolk < uniform < egg-white < egg-shell. This was attributed to the progressive increase of the ratio $Mo_a^{(VI)}/Mo_p^{(VI)}$ which depend on the values of some critical impreg-

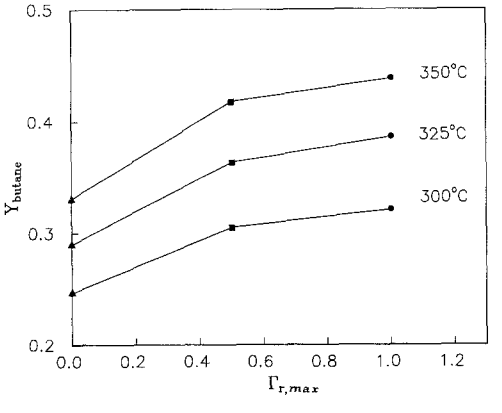


FIG. 19. Dependence of the relative yield of butane on the distance of the maximum of the Mo profile from the periphery of the extrudate ($\Gamma_r = R - r_{max}/R$). The values of temperature are indicated: ●, egg-yolk; ■, egg-white; ▲, egg-shell.

nation parameters (mainly pH) selected for each preparation. The increase in the abovementioned interactions from egg-yolk to egg-shell profile suggested an analogous increase for the $Mo^{(VI)}$ dispersion, and it was confirmed by XPS measurements. The progressive increase in the $Mo^{(VI)}$ dispersion mentioned above was expected to cause an analogous increase in the number of active sites, estimated by the amount of the adsorbed NO. The trend obtained for the latter was similar but not identical to that achieved for the dispersion. The relatively high value obtained for the egg-yolk profile as compared to that obtained for the uniform profile was attributed to the relatively high values of the ratio "tetrahedral Mo/octahedral Mo" assumed for the egg-yolk profile.

d. With the exception of egg-shell profile a very good correlation was observed between the rate of hydrodesulfurization of thiophene and the amount of adsorbed NO, indicating that the activity increases with the number of active sites. The same trend in the rate was obtained over powder and the corresponding extrudate of catalysts. This result suggested that the hds activity of extrudates is mainly determined by the number and quality of active centers and not by the type of the Mo profile. However, the observation that in all cases the value of the rate over powders was higher as compared with the corresponding value in extrudates suggested the presence of appreciable diffusional effects. The trend observed in the values of effectiveness factor, $\eta_{\text{egg-shell}} > \eta_{\text{egg-white}} > \eta_{\text{egg-yolk}}$, was anticipated, whereas the relatively low value obtained for the uniform distribution was attributed to the closing of the pores of the support during Mo deposition.

e. It was found that the relative yield of butane, produced by the hydrogenation of the hds unsaturated products, increased with the distance of the maximum of the Mo profile from the periphery of the extrudate to its center. The relatively low value obtained for the uniform profile was attributed to the forementioned clogging of the pores.

ACKNOWLEDGMENTS

The authors thank Dr. J. M. Palacios (Institutó de Quimica Fisica "Rocasolano," C.S.I.C., Serrano 119, 28006 Madrid, Spain) for SEM-EDX measurements. We also thank Mr. D. Pliatsikas (Department of Chemistry, University of Patras, Patras, Greece) for doing the SSA and TPR experiments.

REFERENCES

1. Goula, M. A., Kordulis, Ch., and Lycourghiotis, A., *J. Catal.* **133,** 486 (1992).
2. Srinivasan, R., Liu, H. C., and Weller, S. W., *J. Catal.* **57,** 87 (1979).
3. Fierro, J. L. G., Grange, P., and Delmon, B., *in* "Preparation of Catalysts VI," p. 591. Elsevier, Amsterdam, 1987.
4. Lee, S. Y., and Aris, R., *Catal. Rev.-Sci. Eng.* **27**(2), 207 (1985).
5. Snell, F. D., "Photometric and Fluorometric Methods of Analysis of Metals," Vol. 2, p. 1296. Wiley, New York, 1978.
6. Lemaitre, J. L., *in* "Characterization of Heterogeneous Catalysts" (F. Delanay, Ed), Chap. 1. Dekker, New York, 1984.
7. Vordonis, L., Koutsoukos, P. G., and Lycourghiotis, A., *J. Catal.* **98,** 296 (1986).
8. Vordonis, L., Koutsoukos, P. G., and Lycourghiotis, A., *J. Catal.* **101,** 186 (1986).
9. Acratopulu, K., Vordonis, L., and Lycourghiotis, A., *J. Chem. Soc. Faraday Trans 1* **82,** 3697 (1986).
10. Spanos, N., Vordonis, L., Kordulis, Ch., and Lycourghiotis, A., *J. Catal.* **124,** 301 (1990).
11. Spanos, N., Vordonis, L., Kordulis, Ch., Koutsoukos, F. G., and Lycourghiotis, A., *J. Catal.* **124,** 315 (1990).
12. Vordonis, L., Koutsoukos, P. G., and Lycourghiotis, A., *Colloids Surf.* **50,** 353 (1990).
13. Spanos, N., Ph.D. Thesis, University of Patras, 1990.
14. Komiyama, M., Merril, R. P., and Harnsberger, H. F., *J. Catal.* **63,** 35 (1980).
15. Lewnard, J. J., Petersen, E. E., and Radke, C. J., *J. Chem. Soc. Faraday Trans. 1* **84** (11), 3927 (1988).
16. Chu, P., Petersen, E. E., and Radke, C. J., *J. Catal.* **117,** 52 (1989).
17. Wagner, C. D., Riggs, W. M., Davis, L. E. Moulder, J. F. and Muilenberg, G. E. (Eds.), "Handbook of X-ray Photoelectron Spectroscopy," Perkin–Elmer, Norwalk, CT, 1979.
18. Kordulis, Ch., Voliotis, S., Lycourghiotis, A., Vattis, D. and Delmon, B., *Appl. Catal.* **11,** 179 (1984).
19. Houalla, M., Kibby, C. L., Petrakis, L., and Hercules, D. M., *J. Catal.* **83,** 50 (1983).
20. Masuyama, Y., Komatsu, Y., Ishida, K., Kurusu, Y., and Segawa, K.-I., *J. Catal.* **114,** 347 (1988).
21. Thomas, R., Van Oers, E. M., de Beer, V. H. J.,

Medema, J. and Moulijn, J. A., *J. Catal.* **76,** 21 (1982).
22. Arnoldy, P., Franken, M. C., Scheffer, B., and Moulijn, J. A., *J. Catal.* **96,** 381 (1985).
23. Ratnasamy, P., Ramaswamy, A. V., Banerjiee, K., Sharma, D. K., and Ray, N., *J. Catal.* **38,** 19 (1975).
24. Chung, K. S., and Massoth, F. E., *J. Catal.* **64,** 320 (1980).
25. Giordano, N., Bart, J. C. J., Castellan, A., and Vaghi, A., *J. Less-Common Met.* **36,** 367 (1974).
26. Chung, K. S., and Massoth, F. E., *J. Catal.* **96,** 122 (1985).
27. Cordero, R. L., Llambias, F. J. G., and Agudo, A. L., *Appl. Catal.* **74,** 125 (1991).
28. Ismail, H. M., Zaki, M. I., Bond, G. C., and Shukri, R., *Appl. Catal.* **72,** L1 (1991).
29. Segawa, K.-I., and Hall, W. K., *J. Catal.* **77,** 221 (1982).
30. O'Young, C.-L., Yang, C.-H., DeCanio, S. J., Patel, M. S., and Storm, D. A., *J. Catal.* **112,** 307 (1988).
31. Caceres, C. V., Fierro, J. L. G., Lopez Agudo, A., Blanco, M. N., and Thomas, H. J., *J. Catal.* **95,** 501 (1985).
32. Okamoto, Y., Katoh, Y., Mori, Y., Imanaka, T., and Teranishi S., *J. Catal.* **70,** 445 (1981).
33. Jung, H. J., Schmitt, J. L., and Ando, H., *in* "Proceedings of the 4th Inter. Conference on the Chemistry and Uses of Molybdenum" (H. F. Barry and P. C. H. Mitchell, Eds.), p. 246. Climax Molybdenum Co., Golden Colorado, 1982.
34. Okamoto, Y., Tomioka, H., Katoh, Y., Imanaka, T., and Terenishi, S., *J. Phys. Chem.* **84** (14), 1833 (1980).
35. Giordano, N., Bart, J. C. J., Vachi, A., Castellan, A., Martinetti, G., *J. Catal.* **36,** 81 (1975).
36. Caceres, C. V., Fierro, J. L. G., Blanco, M. N., and Thomas, H. J., *Appl. Cataly.* **10,** 333 (1984).
37. Weigold, H., *J. Catal.* **83,** 85 (1983).
38. Scheffer, B., Arnoldy, P., and Moulijn, J. A., *J. Catal.* **112,** 516 (1988).
39. Caceres, C. V., Blanco, M. N., and Thomas, H. J., *in* "Preparation of Catalysts III," p. D21. Elsevier, Amsterdam, 1982.
40. Babcock, K. W., Hiltzik, L., Ernst, W. R., and Carruthers, J. D., *Appl. Catal.* **51,** 295 (1989).